Food and Chemical Toxicology 175 (2023) 113741

Contents lists available at ScienceDirect

Food and Chemical Toxicology

journal homepage: www.elsevier.com/locate/foodchemtox

Role of ROS/JAK2/STAT3 signaling pathway in di-n-butyl phthalate-induced testosterone synthesis inhibition and antagonism of lycopene

Qi Wang [a,1], Xia Wu [b,1], Jian Zhang [a], Miao Song [a], Jiayu Du [a], Yilong Cui [c], Yanfei Li [a,*]

[a] Key Laboratory of the Provincial Education, Department of Heilongjiang for Common Animal Disease Prevention and Treatment, College of Veterinary Medicine, Northeast Agricultural University, Harbin, 150030, China
[b] College of Food Science, Northeast Agricultural University, Harbin, 150030, China
[c] College of Animal Science and Technology, Inner Mongolia Minzu University, Tongliao, 028000, China

ARTICLE INFO

Handling Editor: Dr. Bryan Delaney

Keywords:
di-n-butyl phthalate
ROS/JAK2/STAT3 signaling pathway
Testosterone synthesis
Lycopene

ABSTRACT

Di-n-butyl phthalate (DBP) causes adverse effects on male reproduction, especially testosterone synthesis inhibition. However, the specific mechanism of DBP-induced testosterone synthesis inhibition and its effective intervention measures of prevention and treatment are scarce presently. Lycopene (LYC) plays beneficial roles in male infertility because of its antioxidant activity. Nevertheless, it is unclear whether LYC could prevent DBP-induced male reproductive toxicity. By *in vitro* and *in vivo* investigations, this study demonstrated that DBP activated ROS/JAK2/STAT3 signaling pathway, promoted mitophagy and apoptosis, which in turn inhibited testosterone synthesis. Additionally, another major finding was that LYC supplement could reverse the above change, presenting as the restraint of ROS/JAK2/STAT3 signaling pathway, reduction of mitophagy and apoptosis, and improvement of testosterone synthesis. Our study facilitates deeper understandings of the mechanism in DBP-induced testosterone synthesis inhibition, and identifies LYC as the effective prevention and control strategies for DBP poisoning.

1. Introduction

Di-n-butyl phthalate (DBP), one of the most frequently observed phthalate acid esters in the environment, is commonly used as plasticizers, softeners, carriers, and food additives (Feng et al., 2021). With the flexible and durable performance, DBP exists widely in plastic coating, medical devices, drugs, cosmetics, children's toys, and food packaging, which has a very broad range of industrial and commercial applications (Pan et al., 2006). In addition, DBP has been categorized as the top-priority pollutant on the list of the China National Environmental Monitoring Center, European Union, and United States Environmental Protection Agency (Xia et al., 2022). Because of the high lipid-water distribution coefficient, DBP is only physically bounds with the polymeric matrix by non-covalent bonds (Gao and Wen, 2016). As a result, DBP is easily released into the surrounding environment, and entries in the food chain through evaporation, leaching and wear during production, application, and disposal, posing a risk to human health (Katsikantami et al., 2016). DBP is identified as a reproductive and developmental toxicant, and has adverse effects on obesity, reproductive health, thyroid function, and fetal development (Swan et al., 2005; Hauser et al., 2006; Huang et al., 2007). Hence, efficient treatment of DBP is of great urgency.

In general, the testicular tissue is the most vulnerable organ to DBP exposure, and Leydig cells are one of the cells for its action, which secrete most of the circulating testosterone (Källsten et al., 2022). Testosterone is essential to maintain normal testicular descent, urethral

Abbreviations: DBP, di-n-butyl phthalate; LYC, lycopene; ROS, reactive oxygen species; SOD, superoxide dismutase; NAC, N-acetylcysteine; MMP, mitochondrial membrane potential; JAK2, Janus kinase 2; STAT3, signal transducers and activators of transcription 3; IC_{50}, 50% inhibitory concentration; PBS, phosphate-buffered saline; TEM, transmission electron microscope; EB, ethidium bromide; AO, acridine orange; SDS-PAGE, sulfate polyacrylamide gel electrophoresis; PVDF, polyvinylidene fluoride; StAR, steroidogenic acute regulatory protein; CYP11A1, P450 side-chain cleavage enzyme; CYP17A1, 17α-hydroxylase/17, 20 lyase; 3β-HSD, 3 beta-hydroxysteroid dehydrogenase; 17β-HSD, 17 beta-hydroxysteroid dehydrogenase; Cyt-c, cytochrome *c*; SD, standard deviation.

* Corresponding author. College of Veterinary Medicine, Northeast Agricultural University, NO. 600, Changjiang Road, Harbin, 150030, China.
E-mail address: liyanfei@neau.edu.cn (Y. Li).

[1] The authors contributed equally to this study.

https://doi.org/10.1016/j.fct.2023.113741
Received 27 January 2023; Received in revised form 18 March 2023; Accepted 20 March 2023
Available online 21 March 2023

opening, and sperm formation (Basaria et al., 2001). Insufficient levels of testosterone in males are linked with a wide range of disorders such as osteoporosis, infertility, bone loss, and diabetes (Elmigdadi et al., 2005; Tuck and Francis, 2009; Yarrow et al., 2017). DBP has been shown to be environmental endocrine disruptors with antiandrogenic properties and a more pronounced effect in males, and also induces oxidative stress (Guo et al., 2014). Oxidative stress brings about a decline in the levels of reproduction-related critical cell-cycle factors, and directly damage multiple intracellular components, such as DNA, proteins, and lipids (Lord and Aitken, 2013). In addition, DBP and its metabolites inhibit the synthesis of testosterone through restraining cholesterol transport, and the enzymes related to testosterone synthesis (Johnson et al., 2011). As an important cytokine signal transduction pathway, the Janus kinase 2 (JAK2)/signal transducers and activators of transcription 3 (STAT3) serves as a vital role in many pathological and physiological processes, which is also related to cell differentiation, proliferation, oxidative stress, and apoptosis (Li et al., 2018). Multiple studies have found that JAK2/STAT3 signaling pathway is also implicated in male reproductive events, such as sexual development, gametogenesis generation, spermatogonial stem cells renewal, and sperm maturation (Khashab et al., 2021). Accordingly, it could be a potential novel target to investigate the effect of DBP on testosterone synthesis from the perspective of oxidative stress and JAK2/STAT3 signaling pathway.

Lycopene (LYC), a type of fat-soluble natural carotenoid, is listed as a food colorant by the Joint Food and Agriculture Organization/World Health Organization Expert Committee on Food Additives, which is usually found in red fruit and vegetables including tomatoes, watermelons, red peppers, and papayas (Wang et al., 2019). Since LYC is only synthesized by plants and microorganisms, neither by animal or human, it must be accessible from a variety of dietary sources (Cao et al., 2021). LYC is readily absorbed by the body, and preferentially accumulates in livers, adrenal glands, and prostate glands, with up to 10 times higher concentrations in the testes than other tissues (Petyaev, 2016). What's more, LYC has numerous biological effects, such as anticancer, antioxidation, anti-inflammation, cardioprotective, and anti-apoptosis (Bandeira et al., 2017; Li et al., 2017; Costa-Rodrigues et al., 2018). LYC has been established to reduce lipid peroxidation, abate reactive oxygen species (ROS) burden and the number of free radicals, thereby alleviating oxidative stress in the reproductive organs, thus mitigating testicular toxicity (Durairajanayagam et al., 2014). Nevertheless, exactly whether LYC could ameliorate DBP-induced male reproductive toxicity, and its specific protective mechanisms remain a mystery. The objectives of present study were to give a deeper insight into mechanisms of DBP-induced testosterone synthesis inhibition, and find a natural dietary compound to provide a strategy for the prevention and treatment of DBP poisoning.

2. Materials and methods

2.1. TM3 cell culture

The mouse Leydig (TM3) cell lines were a kind gift from Professor Miao Long (Shenyang Agricultural University, China). TM3 cells were incubated in sterile DME/F-12 medium (CGM104.05, Cellmax, China) with 10% fetal bovine serum (SA211.02, Cellmax, China), supplemented with 100 units/mL penicillin, and 100 units/mL streptomycin (C0222, Beyotime, China). Cells were cultured in a humidified atmosphere containing 5% CO_2 inncubator at 37 °C (QP-160, Biobase, China).

2.2. Cell experimental procedure

Above all, all the stock solutions were prepared, lysed by ultrasonic, stored at −20 °C, and diluted with medium according to the need of experiment for further use. 530 μL DBP (purity >99.5%, D806671, Macklin, China) was mixed with 1 mL DMSO (ST038, Beyotime, China), and then diluted 10-fold with cell culture medium to reach a concentration of 200 mM. 234 mg NAC (purity ≥99%, ST1546, Beyotime, China) was dissolved in 2.87 mL cell culture medium to reach a concentration of 500 mM. 25 mg AG490 (purity = 99.66%, A4139, APExBIO, USA) was dissolved in 1.7 mL DMSO to reach a concentration of 50 mM. 20 mg LYC (purity ≥90%, B20378, Yuanye Bio-Technology, China) was dissolved in 3.72 mL DMSO to reach a concentration of 10 mM.

Afterwards, to screen the optimal doses for the experiments, the TM3 cells were treated with concentration gradient of DBP (10, 100, 200, 400, 800, 1600 μM), AG490 (5, 10, 15, 20, 25, 30, 35, 40 μM), and LYC (10, 20, 30, 40, 50, 60, 70 μM) respectively for CCK-8 detections. After 24 h-DBP exposure, results showed that the cell viability was near 50% inhibitory concentration (IC_{50}) at 200 μM. To achieve obvious treatment and intervention effect, we chose the highest doses of AG490 and LYC that did not significantly affect the cell viability. Therefore, 15 μM AG490 and 20 μM LYC were selected in the subsequent experiment. Additionally, based on previous studies, we chose 5 mM NAC for further experiments (Sun et al., 2018a). And then three *in vitro* experiments were conducted in turn.

NAC-intervention experiment: the administration groups were marked as Control, NAC (5 mM), DBP (200 μM), and DBP + NAC. The Control group was treated with DME/F-12 medium only, whereas other groups were administrated with DBP or/and NAC for 24 h.

AG490-intervention experiment: the administration groups were marked as Control, AG490 (15 μM), DBP (200 μM), and DBP + AG490. Before 24 h-exposure of DBP, AG490 was pretreated for 1 h. The Control group was administrated with DME/F-12 medium only.

LYC-treatment experiment: the administration groups were marked as Control, LYC (20 μM), DBP (200 μM), and DBP + LYC. The Control group was treated with DME/F-12 medium only, whereas other groups were administrated with DBP or/and LYC for 24 h.

2.3. Animal and experimental procedure

Fifty SPF grade male C57BL/6N mice at 6 weeks (18−21 g) of age were purchased from Liaoning Changsheng Biotechnology Co., Ltd. (Benxi, Liaoning, China). All animal use and procedures in the current study were carried out under the permission of the Animal Ethics Committee of Northeast Agricultural University. The basic principles of experimental animal welfare were strictly observed. Adaptive housing for 1 week prior before the experiment. The mice were provided with free access to standard laboratory food and distilled water, set at 22–25 °C with a relative humidity of 50–70% and 12 h/12 h light/dark cycle. And then, the experimental mice were randomly divided into the following five groups (10 mice per group):

Control group: 0.1 mL corn oil, oral gavage, once a day, at 10:00 a.m. daily.

DBP group: DBP (250 mg/kg of body weight, at 13:00 p.m.), oral gavage, once a day.

DBP + NAC group: NAC (200 mg/kg of body weight, 10:00 a.m.) plus DBP (250 mg/kg of body weight, at 13:00 p.m.), oral gavage, once a day.

DBP + AG490 group: AG490 (10 mg/kg of body weight, 10:00 a.m., intraperitoneal injection, once every two days) plus DBP (250 mg/kg of body weight, at 13:00 p.m., oral gavage, once a day).

DBP + LYC group: LYC (10 mg/kg of body weight, 10:00 a.m.) plus DBP (250 mg/kg of body weight, at 13:00 p.m.), oral gavage, once a day.

DBP and LYC were dissolved in corn oil. NAC was dissolved in sterile water. AG490 was first dissolved in DMSO (5% (v/v)), and then diluted in sterile water (95% (v/v)). Gavage and injected doses of these reagents were adjusted to a same volume of 0.1 mL per mouse according to the body weight every 5 d. The administration dose of DBP, NAC, AG490, and LYC was based on the previous study and report (Ignarro et al., 2013; Ma et al., 2021; Nakhaee et al., 2021; Meng et al., 2022). After 28 days, mice were euthanized by CO_2 inhalation, blood and testis samples were obtained for analyses.

2.4. Cell viability assay

The CCK-8 assay (K1018, APExBIO, USA) was used to measure the viability of TM3 cells. First, being Seeded in 96-well plates (1×10^4 cells per well), TM3 cells were cultured to 70−80% confluence at environment of 37 °C, 5% CO_2. Then, TM3 cells were exposed to DBP (200 μM) and/or LYC (20 μM) for 24 h. The cell culture medium was discarded in each well, and washed with phosphate-buffered saline (PBS) three times, after which 100 μL new medium and 10 μL CCK-8 solution were added to each well. After being incubated at 37 °C for 1 h, the absorbance of CCK-8 was represented at 450 nm tested by a Tecan Sunrise microplate reader.

2.5. Determination of TM3 cellular and testicular ROS level

Seeded in 24-well plates (2×10^5 cells per well), TM3 cells were respectively exposed to DBP (200 μM) and/or LYC (20 μM) with or without NAC (5 mM) for 24 h to evaluate the intracellular ROS level. After the cell culture medium was removed, cells were incubated with the DCFH-DA probe (WLA131a, Wanleibio, China) for 20 min at 37 °C in the dark. Intracellular ROS were marked by green fluorescent light in the fluorescence microscopy (Eclipse-Ti, Niko, Japan).

Selected testicular tissues (50 mg) were immediately put into the pre-cooled PBS for cleaning, and cut into small pieces. The digestion was carried out using appropriate enzyme digestion solution for 20 min at 37 °C under water bath conditions, and terminated with PBS. Cells were filtered with 300 mesh nylon mesh, and collected to centrifuged at 500 g for 10 min. Collected cell precipitates were resuspended in PBS, and used for measurement (WLA131a, Wanleibio, China). Fluorescence intensities were measured using a fluorescence reader (M200 Pro, Tecan, Switzerland) with a 488 nm excitation and 525 nm emission.

2.6. Measurement of TM3 cellular and testicular SOD level

Seeded in 96-well plates (1×10^4 cells per well), TM3 cells were exposed to DBP (200 μM) and/or LYC (20 μM) with or without NAC (5 mM) for 24 h. Following treatment, cells and testicular tissues (50 mg) were homogenized with PBS. Homogenates were centrifuged at 600 g for 15 min at 4 °C, and the supernatant was gathered. The absorbance was assessed at 550 nm by superoxide dismutase (SOD) detection kits (WLA110b, Wanleibio, China).

2.7. Detection of TM3 cellular and testicular MMP

Seeded in 24-well plates (2×10^5 cells per well), TM3 cells were exposed to DBP (200 μM) and/or AG490 (15 μM) for 24 h. Before 24 h-exposure of DBP, AG490 was pretreated for 1 h. Washed the cells with PBS. 0.5 mL complete culture medium and 0.5 mL JC-1 staining working solution were added into the TM3 cells (C2006, Beyotime, China). After being incubated at 37 °C for 20 min in the dark, discarded the supernatant, washed twice with JC-1 staining buffer, and added 0.2 mL complete culture medium. The mitochondrial membrane potential (MMP) pictures were photographed by a fluorescence microscopy (Eclipse-Ti, Niko, Japan).

Testicular mitochondria were isolated from testicular tissues (50 mg) by using a tissue mitochondrial isolation kit (C3606, Beyotime, China). The MMP of the testicular mitochondria was measured by JC-1 staining (C2006, Beyotime, China). Fluorescence intensities were measured using a fluorescence reader (M200 Pro, Tecan, Switzerland) with a 485 nm excitation and 590 nm emission.

2.8. TM3 cellular EB/AO staining

In order to investigate the morphologies of apoptotic cells altered cell, ethidium bromide (EB)/acridine orange (AO) staining (BB-4132, BestBio, China) was carried out. AO penetrates all intact cell membranes, making nuclei appear green. Once the integrity of the cytoplasmic membrane is lost, EB permeates the cells and stains the nucleus red. Seeded in 24-well plates (2×10^5 cells per well), TM3 cells were exposed to DBP (200 μM) and/or AG490 (15 μM) with or without LYC (20 μM) for 24 h. Before 24 h-exposure of DBP, AG490 was pretreated for 1 h. After washed with PBS twice, 0.5 mL staining buffer, 5 μL EB staining solution, and 5 μL AO staining solution were added in each well, and then incubated at 4 °C for 20 min in the dark. The cellular morphology was examined by a fluorescence microscopy (Eclipse-Ti, Nikon, Japan).

2.9. Testicular TUNEL staining

The whole testicular tissue was removed, fixed in 4% paraformaldehyde, dehydrated in ethanol, cleared using xylene, embedded in resin, and then sectioned. Apoptosis of testicular tissues was performed using TUNEL cell apoptosis detection kit (WLA029b, Wanleibio, China) according to the manufacturer's instructions. Normal cells have blue nuclei, while apoptotic cells have brown nuclei. The sections were observed by a digital section scanner at × 200 magnification (Pannoramic MIDI, Hungary).

2.10. Observation of TM3 cellular ultrastructure

Seeded in 12-well plates (3×10^5 cells per well), TM3 cells were exposed to DBP (200 μM) and/or LYC (20 μM) for 24 h. Following treatment, cells were fixed with 2.5% glutaraldehyde-PBS solution at 4 °C overnight. Then the samples were washed with 0.1 M PBS, fixed with 1% osmic acid, and washed with 0.1 M PBS again, and then dehydrated with gradient alcohol and 100% acetone. After that, samples were embedded in resin, stained, cut into sections, and then imaged using a transmission electron microscope (TEM) (HT7650, Hitachi, Japan).

2.11. Measurement of TM3 cellular and testicular testosterone contents

TM3 cells were exposed to DBP (200 μM) and/or LYC (20 μM) for 24 h in T25 cell culture flasks. The blood samples were collected from mice, and centrifuged at 1500 g for 10 min at 4 °C to obtain the serum. Then, culture supernatants from TM3 cells and the mouse serum were collected to detect testosterone contents using an Iodine[^{125}I] Testosterone Radioimmunoassay Kit (Beijing North Institute of Biotechnology *Co.,Ltd*, China). Data were detected using the ν-radioimmunoanalyzer (FMQ-9013C, Tangshan Chenxi electronics *Co.*, *Ltd*, China), and calculated utilizing a log-logit transformation.

2.12. Western blot analysis of TM3 cells and testicular tissues

Cells were grown in T75 flask, and treated with different agents according to different experimental groups. Total proteins of TM3 cells and testicular tissues (50 mg) were extracted using the strong RIPA cracking solution kit (P0013B, Beyotime, China). The total-protein concentration was detected through enhanced BCA protein assay kit (P0010S, Beyotime, China). Meanwhile, the protein was denatured with 5 × loading buffer at 100 °C for 10 min, which were then separated through 12% sodium dodecyl sulfate polyacrylamide gel electrophoresis (SDS-PAGE). Afterwards, the proteins were electrotransferred onto polyvinylidene fluoride (PVDF) membranes. Subsequently, after being blockaded for 10 min with the pre-treatment solution (M01013, GenScript, China), the protein membranes were immunodetected with primary antibodies against steroidogenic acute regulatory protein (StAR) (sc-166,821, Santa Cruz Biotechnology, USA, 1:500), P450 side-chain cleavage enzyme (CYP11A1) (A1713, ABclonal, China, 1:1000), 17α-hydroxylase/17,20 lyase (CYP17A1) (A5067, ABclonal, China, 1:1000), 3 beta-hydroxysteroid dehydrogenase (3β-HSD) (sc-515,120, Santa Cruz Biotechnology, USA, 1:500), 17 beta-hydroxysteroid dehydrogenase

(17β-HSD) (sc-376,719, Santa Cruz Biotechnology, USA, 1:500), JAK2 (WL02188, Wanleibio, China, 1:500), p-JAK2 (WL02997, Wanleibio, China, 1:500), STAT3 (WL01836, Wanleibio, China, 1:500), p-STAT3 (WLP2412, Wanleibio, China, 1:1000), HSP60 (WL03647, Wanleibio, China, 1:1000), TOM20 (WL03626, Wanleibio, China, 1:500), Beclin-1 (WL02508, Wanleibio, China, 1:500), LC3 II (WL05106, Wanleibio, China, 1:500), Bax (WL01637, Wanleibio, China, 1:500), Bcl-2 (WL01556, Wanleibio, China, 1:500), cytochrome *c* (Cyt-c) (WL02410, Wanleibio, China, 1:1000), and cleaved-caspase-3 (WL04004, Wanleibio, China, 1:500). After being washed with PBST, the membranes were incubated with secondary antibodies (M20027XS and M21002S, Abmart, China, 1: 5000) for 1 h at 37 °C to carry out an enhanced ECL reagent reaction (P0018S, Beyotime, China). GAPDH (MA000071M1m, Cusabio, China, 1:15,000) was detected as controls. All protein data were normalized to the Control group, which was set as 100% by using Amersham Imager 600 (General Electric, Fairfield, USA).

2.13. Statistical analyses

The numerical results are presented as the mean ± standard deviation (SD) from at least three independent experiments. Statistical analysis was performed by single-factor variance analysis using the SPSS 22.0 statistical software. The experimental data were analyzed by using the GraphPad Prism 5.0 software. The significance was considered at the probability level of $P < 0.05$ and $P < 0.01$. The data were marked as $*/\#P < 0.05$, and $**/\#\#P < 0.01$.

3. Results

3.1. Effects of NAC intervention on the oxidative stress and JAK2/STAT3 signaling pathway in DBP-exposed TM3 cells

After DBP exposure, the TM3 cell viability exhibited a concentration-dependent attenuation when compared to the Control level. It was calculated that IC_{50} of 24 h-DBP-exposed TM3 cells was 236 μM. Considering that the cell viability was nearly 50% of the level in Control group when the concentration of DBP was 200 μM, we chose it as the experimental concentration of DBP (Fig. 1A). It was also shown that the solvent DMSO had no significant effect on the TM3 cell viability (Fig. 1B). The ROS level was significantly ($P < 0.01$) augmented in the DBP group when compared with the levels in the Control group. While the ROS level was significantly ($P < 0.01$) attenuated in the DBP + NAC group when compared to the level of DBP group (Fig. 1C). Moreover, DBP administration significantly ($P < 0.01$) reduced the SOD activity compared with the Control groups. Whereas the SOD activity was significantly ($P < 0.01$) higher in the DBP + NAC group than in the DBP group (Fig. 1D). In addition, the ratios of p-JAK2/JAK2 and p-STAT3/STAT3 exhibited a significant ($P < 0.01$) elevation in the DBP group when compared to the Control group. The ratios of p-JAK2/JAK2 and p-STAT3/STAT3 showed a significant ($P < 0.01$) down-regulation among DBP and NAC treated cells when compared with the DBP-exposed cells (Fig. 1E).

3.2. Effects of AG490 intervention on the testosterone content and JAK2/STAT3 signaling pathway and in DBP-exposed TM3 cells

Compared to the Control group, the TM3 cell viability exhibited a concentration-dependent attenuation after AG490 exposure. When the concentration of AG490 was ≥30 μM, the viability of TM3 cells decreased significantly ($P < 0.01$) (Fig. 2A). Finally, we chose 15 μM as the experimental concentration of AG490, in which there was no significant difference as compared to the Control group. Exposure to DBP obviously ($P < 0.01$) decreased the testosterone content relative to the levels in the Control group. The intervention of AG490 significantly ($P < 0.01$) promoted testosterone content relative to DBP-group cells (Fig. 2B). Additionally, the ratios of p-JAK2/JAK2 and p-STAT3/STAT3 exhibited a significant ($P < 0.01$) elevation in the DBP group when compared to the Control group. The ratios of p-JAK2/JAK2 and p-STAT3/STAT3 showed a significant ($P < 0.01$) down-regulation among DBP and AG490-treated cells when compared with the DBP-exposed cells (Fig. 2C).

3.3. Effects of AG490 intervention on the mitophagy and apoptosis of DBP-exposed TM3 cells

After DBP exposure, a significantly ($P < 0.01$) increased ratio of green and red fluorescence of JC-1 was present when compared with the Control group. The DBP and AG490 administration in TM3 cells provided a significant ($P < 0.01$) reduction in the ratio of green and red fluorescence of JC-1 when compared to the DBP-exposed cells (Fig. 2D). LC3 II and Beclin-1 protein levels were significantly ($P < 0.01$) increased in the DBP group as compared with the levels in the Control group, and significantly ($P < 0.01$) decreased in the DBP + AG490 group as compared with the levels in the DBP group. HSP60 and TOM20 protein

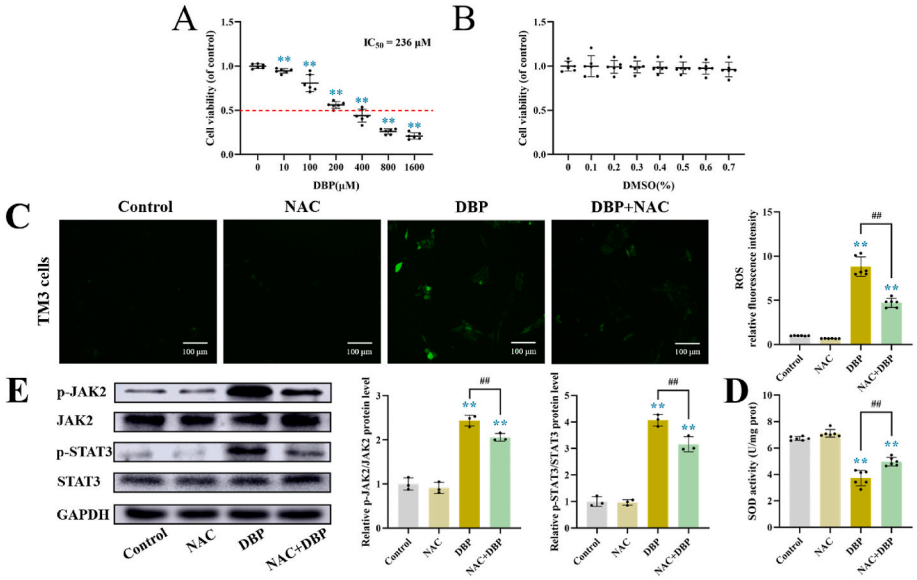

Fig. 1. Effects of NAC intervention on the oxidative stress and JAK2/STAT3 signaling pathway in DBP-exposed TM3 cells. (A) TM3 Cell viability when exposed to concentration gradients of DBP. (B) TM3 Cell viability when exposed to different proportions of DMSO. (C) ROS level. (D) SOD activity. (E) Protein levels of p-JAK2, JAK2, p-STAT3, and STAT3. GAPDH was served as protein loading controls. All protein data were normalized to the Control group, which was set as 100%. Data are presented as mean ± SD. Each set of experiments was repeated three times. * and # ($P < 0.05$), ** and ## ($P < 0.01$).

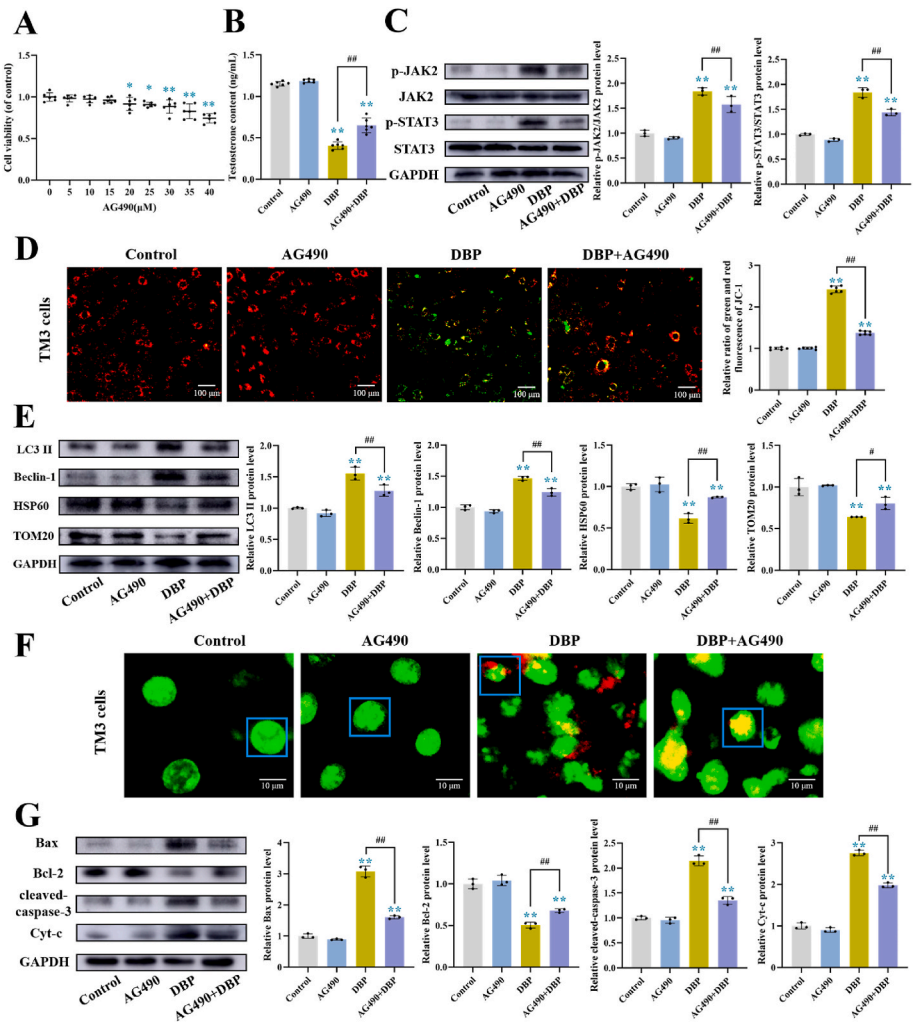

Fig. 2. Effects of AG490 intervention on the testosterone content, JAK2/STAT3 signaling pathway, mitophagy, and apoptosis in DBP-exposed TM3 cells. (A) TM3 Cell viability when exposed to concentration gradients of AG490. (B) Testosterone content. (C) Protein level of p-JAK2, JAK2, p-STAT3, and STAT3. (D) MMP level. (E) Protein level of LC3 II, Beclin-1, HSP60, and TOM20. (F) EB/AO staining. (G) Protein levels of Bax, Bcl-2, cleaved-caspase-3, and Cyt-c. GAPDH was served as protein loading controls. All protein data were normalized to the Control group, which was set as 100%. Data are presented as mean ± SD. Each set of experiments was repeated three times. * and # ($P < 0.05$), ** and ## ($P < 0.01$).

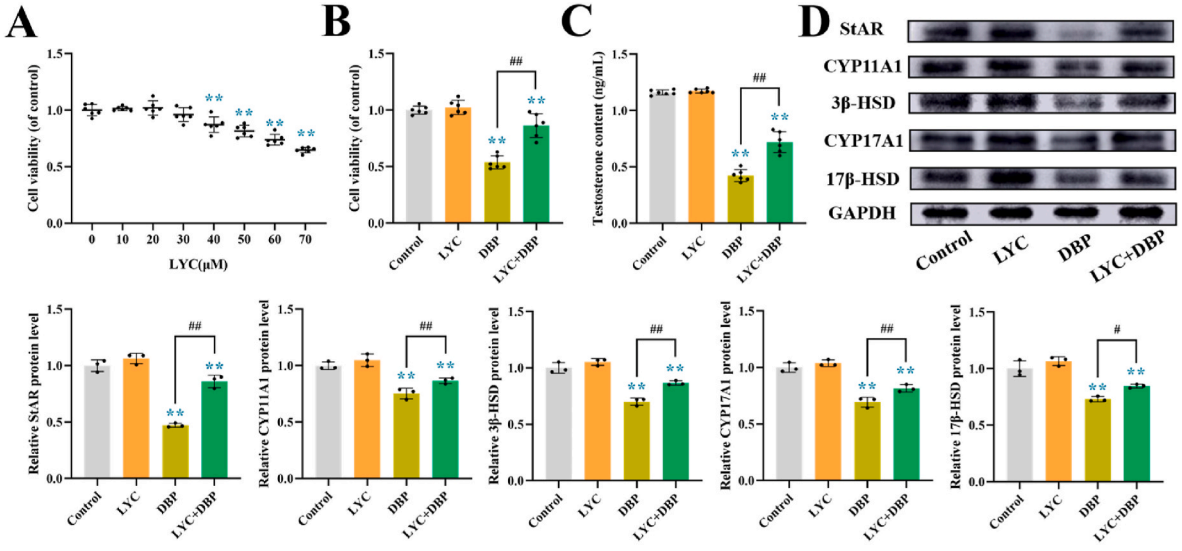

Fig. 3. Effects of LYC treatment on the cell viability and the testosterone synthesis of DBP-exposed TM3 cells. (A) TM3 Cell viability when exposed to concentration gradients of LYC. (B) TM3 cell viability. (C) Testosterone content. (D) Protein levels of StAR, CYP11A1, 3β-HSD, CYP17A1, 17β-HSD, and STAT3. GAPDH was served as protein loading controls. All protein data were normalized to the Control group, which was set as 100%. Data are presented as mean ± SD. Each set of experiments was repeated three times. * and # ($P < 0.05$), ** and ## ($P < 0.01$).

levels were obviously ($P < 0.01$) reduced in the DBP group relative to the Control group, and significantly ($P < 0.01$) enhanced in the DBP + AG490 group relative to DBP-group level (Fig. 2E).

After EB/AO double fluorescent labeling, green colorizations with regular nuclei were noticed in the Control-group cells. Compared with DBP-group cells, the TM3 cells treated with DBP and AG490 had an obvious promotion of cell viabilities, and relieved apoptosis-induced morphological alterations such as severe yellow to green colorization with fragmented nuclei and condensed chromatin, and red colorization with fragmented nuclei (Fig. 2F). The DBP group showed a significant ($P < 0.01$) upregulation of cleaved-caspase-3, Cyt-c, and Bax protein expressions, and a significant ($P < 0.01$) downregulation of Bcl-2 protein expression, relative to the Control group. The cleaved-caspase-3, Cyt-c, and Bax protein levels were observably ($P < 0.01$) decreased, while the level of Bcl-2 was observably ($P < 0.01$) increased in the DBP + AG490 group relative to BP group (Fig. 2G).

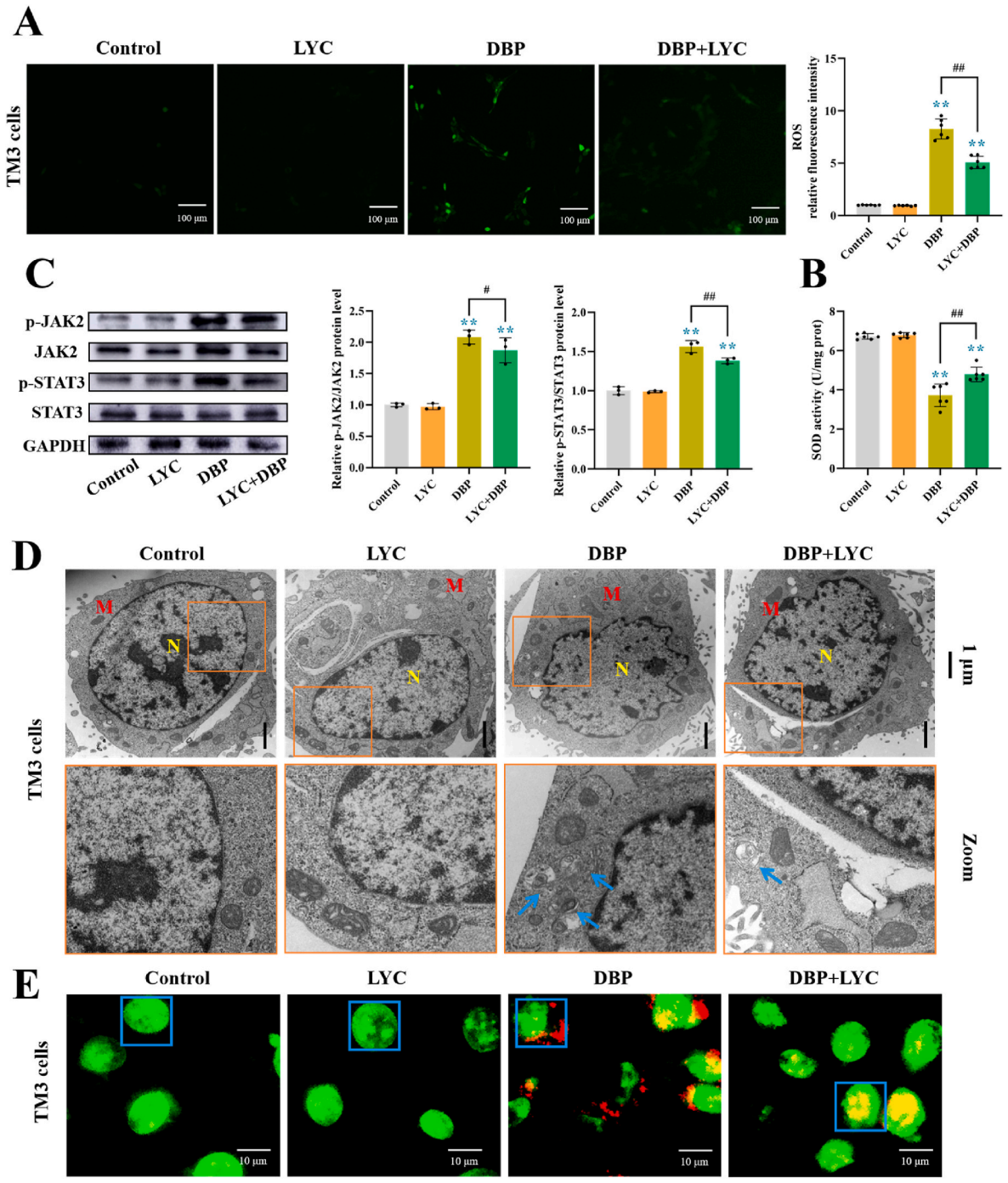

Fig. 4. Effects of LYC treatment on the oxidative stress, JAK2/STAT3 signaling pathway, mitophagy, and apoptosis the of DBP-exposed TM3 cells. (A) ROS level. (B) SOD activity. (C) Protein levels of p-JAK2, JAK2, p-STAT3, and STAT3. (D) Transmission electron microscopy of TM3 cells. The yellow N indicates nuclei. The red M indicates mitochondria. The blue arrows indicate mitophagosomes. (E) EB/AO staining. All protein data were normalized to the Control group, which was set as 100%. GAPDH was served as protein loading controls. Data are presented as mean ± SD. Each set of experiments was repeated three times. * and # ($P < 0.05$), ** and ## ($P < 0.01$). (For interpretation of the references to color in this figure legend, the reader is referred to the Web version of this article.)

3.4. Effects of LYC treatment on cell viability and the testosterone synthesis in DBP-exposed TM3 cells

As LYC concentration increased, the cell viability first increased and then decreased when compared to Control-group cells. Considering that the cell viability had no significant difference and peaked relative to the Control level at the concentration of 20 μM, we chose it as the subsequent experimental concentration of LYC (Fig. 3A). In the LYC-treatment experiment, the TM3 cell viability were significantly declined in the DBP-exposed group, whereas the TM3 cell viability was significantly ($P < 0.01$) enhanced after LYC treatment (Fig. 3B). Besides, there was no significant difference in the levels of testosterone content and testosterone synthetase-associated proteins between the Control and LYC groups. Exposure to DBP obviously ($P < 0.01$) decreased the testosterone content relative to the Control group. The treatment of LYC significantly ($P < 0.01$) promoted testosterone content relative to DBP-group cells (Fig. 3C). Furthermore, the StAR, CYP11A1, CYP17A1, 3β-HSD, and 17β-HSD protein levels were significantly ($P < 0.01$) lower in the DBP-exposed cells relative to the Control levels. The levels of testosterone synthetase-associated proteins were observably ($P < 0.01$) promoted after LYC treatment relative to levels in the DBP group (Fig. 3D).

3.5. Effects of LYC treatment on the oxidative stress, JAK2/STAT3 signaling pathway, mitophagy, and apoptosis in DBP-exposed TM3 cells

The DBP group exhibited a marked ($P < 0.01$) rise of ROS level compared with the Control group. The DBP + LYC group showed a marked decrease of the ROS level when compared to the level of DBP group ($P < 0.01$) (Fig. 4A). Moreover, SOD activities were obviously ($P < 0.01$) decreased in the TM3 cells treated with DBP relative to the Control group, whereas were obviously ($P < 0.01$) higher in the DBP + LYC group than that in the DBP group (Fig. 4B). In addition, the ratios of p-JAK2/JAK2 and p-STAT3/STAT3 exhibited a significant ($P < 0.01$) elevation in the DBP group when compared to the Control group. The ratios of p-JAK2/JAK2 and p-STAT3/STAT3 showed a significant ($P < 0.05$, $P < 0.01$) down-regulation among DBP and LYC-treated cells when compared with the DBP group (Fig. 4C).

As shown in the TEM examination, the Control group and LYC group showed the normal ultrastructure of cellular mitochondrion, and well-arranged mitochondria with intact membranes and dense cristae. In contrast, the DBP-exposed group showed the swelled and vacuolar mitochondrion, the dissolved cristae of mitochondrial, and abnormal mitochondrial autophagic vesicle. After LYC treatment, those pathological changes had improved (Fig. 4D). After EB/AO double fluorescent labeling, green colorizations with regular nuclei were noticed in the Control-group cells. Compared with DBP-group cells, the TM3 cells treated with DBP and LYC had an obvious promotion of cell viabilities, and relieved apoptosis-induced morphological alterations such as severe yellow to green colorization with fragmented nuclei and condensed chromatin, and red colorization with fragmented nuclei (Fig. 4E).

3.6. Effects of NAC intervention and LYC treatment on the oxidative stress, JAK2/STAT3 signaling pathway in DBP-exposed mouse testes

The ROS level was significantly ($P < 0.01$) augmented in the DBP group when compared with the level in the Control group. While the ROS level was significantly ($P < 0.01$) attenuated both in the DBP + NAC group and DBP + LYC group when compared to the level of DBP group (Fig. 5A). Moreover, DBP administration significantly ($P < 0.01$) reduced the SOD activity compared with the Control groups. Whereas the SOD activity was significantly ($P < 0.01$) higher in both DBP + NAC group and DBP + LYC group than in the DBP group (Fig. 5B). In addition, the ratios of p-JAK2/JAK2 and p-STAT3/STAT3 exhibited a significant ($P < 0.01$) elevation in the DBP group when compared to the Control group. The ratios of p-JAK2/JAK2 and p-STAT3/STAT3 showed a significant ($P < 0.01$) down-regulation in both DBP + NAC group and DBP + LYC group when compared with the DBP-exposed group (Fig. 5C).

3.7. Effects of AG490 intervention and LYC treatment on JAK2/STAT3 signaling pathway, mitophagy, and apoptosis in DBP-exposed mouse testes

The ratios of p-JAK2/JAK2 and p-STAT3/STAT3 exhibited a significant ($P < 0.01$) elevation in the DBP group when compared to the Control group. The ratios of p-JAK2/JAK2 and p-STAT3/STAT3 showed a significant ($P < 0.01$) down-regulation in the DBP + AG490 group and DBP + LYC group when compared with the DBP group (Fig. 5D). After DBP exposure, a significantly ($P < 0.01$) increased ratio of green and red fluorescence of JC-1 was present when compared with the Control group. The DBP + AG490 group and DBP + LYC group provided a significant ($P < 0.01$) reduction in the ratio of green and red fluorescence of JC-1 when compared to the DBP-exposed group (Fig. 5E). LC3 II and Beclin-1 protein levels were significantly ($P < 0.01$) increased in the DBP group as compared with the levels in the Control group, and significantly ($P < 0.01$) decreased in the DBP + AG490 group and DBP + LYC group as compared with the levels in the DBP group. The HSP60 and TOM20 protein levels were obviously ($P < 0.01$) reduced in the DBP group relative to the Control level, and significantly ($P < 0.01$) enhanced in the DBP + AG490 group and DBP + LYC group relative to DBP-group level (Fig. 5F). As shown in the TUNEL staining, DBP group had an obvious augment of apoptotic Leydig cells when compared with the Control group ($P < 0.01$). The DBP + AG490 group and DBP + LYC group had an obvious reduction of apoptotic Leydig cells when compared with the DBP-exposed group ($P < 0.01$) (Fig. 5G). The DBP group showed a significant ($P < 0.01$) upregulation of cleaved-caspase-3, Cyt-c, and Bax protein expressions, and a significant ($P < 0.01$) downregulation of Bcl-2 protein expression, relative to the Control group. The levels of cleaved-caspase-3, Cyt-c, and Bax proteins were observably ($P < 0.01$) decreased, while the level of Bcl-2 was observably ($P < 0.01$) increased in the AG490 + DBP group and DBP + LYC group relative to the DBP group (Fig. 5H).

3.8. Effects of AG490 intervention and LYC treatment on the testosterone synthesis in DBP-exposed mouse testes

The StAR, CYP11A1, CYP17A1, 3β-HSD, and 17β-HSD protein levels were significantly ($P < 0.01$) lower in the DBP-exposed cells relative to the Control levels. The levels of testosterone synthetase-associated proteins were observably ($P < 0.01$) promoted after AG490 intervention and LYC treatment relative to levels in the DBP group (Fig. 5I). Exposure to DBP obviously ($P < 0.01$) decreased the testosterone content relative to the Control group. The AG490 intervention and LYC treatment significantly ($P < 0.01$) promoted testosterone content relative to DBP-group cells (Fig. 5J).

4. Discussion

DBP is a ubiquitous reproductive toxicant and environmental endocrine disruptors that adversely affects the male health. Although many researchers have evaluated the effect of DBP on reproductive functional changes *in vitro* and *in vivo*, DBP is still the most commonly used plasticizer for its stability, agglutinating value, and waterproofing quality (Wine et al., 1997). The synthesis and secretion of testosterone requires the normal expression of a series of enzymes, including CYP11A1, 17β-HSD, CYP17A1, 3β-HSD, and StAR, which respectively plays a role in the transformation of cholesterol, pregnenolone, progesterone, androstenedione, and testosterone (Midzak et al., 2009; Han et al., 2018). These enzymes expression can be affected by numerous endocrine disruptors, which interferes with the testosterone synthesis. Studies have shown that DBP can disrupt testosterone synthesis in the testes. Zhang et al. have demonstrated that the serum testosterone production of prepubertal male rats is inhibited when exposed to 0, 250, 500, 1000, and 2000 mg/kg DBP daily for 30 days (Zhang et al., 2009). Duan et al.

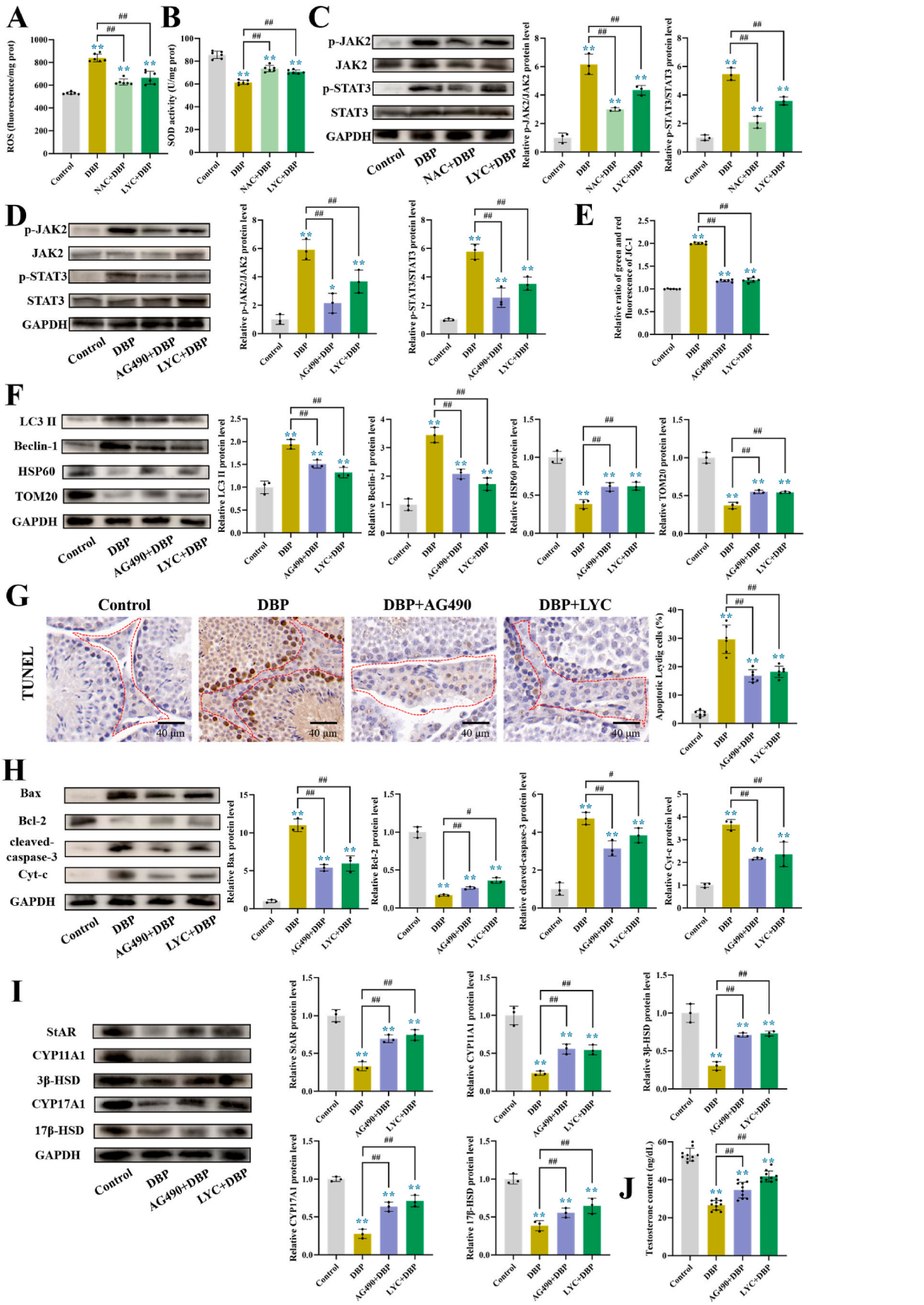

(caption on next page)

Fig. 5. Effect of ROS/JAK2/STAT3 signaling pathway and LYC antagonistic activities on DBP-induced testosterone synthesis inhibition in mice. (A) ROS level. (B) SOD activity. (C) Protein levels of p-JAK2, JAK2, p-STAT3, and STAT3. (D) Protein levels of p-JAK2, JAK2, p-STAT3, and STAT3. (E) MMP level. All treatment group were normalized to the Control group, which was set as 100%. (F) Protein levels of LC3 II, Beclin-1, HSP60, and TOM20. (G) TUNEL staining of testis sections. The interstitial area of the testis is encircled in red dotted lines. (H) Protein levels of Bax, Bcl-2, cleaved-caspase-3, and Cyt-c. (I) Protein levels of StAR, CYP11A1, 3β-HSD, CYP17A1, 17β-HSD, and STAT3. (J) Testosterone content. All protein data were normalized to the Control group, which was set as 100%. GAPDH was served as protein loading controls. Data are presented as mean ± SD. Each set of experiments was repeated three times. * and # ($P < 0.05$), ** and ## ($P < 0.01$). (For interpretation of the references to color in this figure legend, the reader is referred to the Web version of this article.)

have demonstrated that di (2-ethylhexyl) phthalate, DBP, and bis (2-ethylhexyl) adipate alter the expression levels of some key proteins in steroidogenesis pathways, thereby directly or indirectly affecting the secretion of testosterone in H295R cells (Duan et al., 2020). Thompson et al. have found that DBP exposure leads to diminution of the expression of several proteins required for cholesterol transport and steroidogenesis in the fetal testis, resulting in decreased testosterone synthesis, and consequent male reproductive maldevelopment (Thompson et al., 2004). Chen et al. have shown that the testosterone secretion is inhibited when the murine Leydig tumor cell line MLTC-1 were incubated with higher treatment doses of DBP (100 μmol/L in DMSO) (Chen et al., 2013). And our results reconfirmed these findings, DBP exposure reduced the testosterone content and the protein expressions of CYP11A1, 17β-HSD, CYP17A1, 3β-HSD, and StAR both in TM3 cells and mouse testes, suggesting that DBP induced testosterone synthesis inhibition *in vitro* and *in vivo*. In this study, to explore the exact mechanism by which DBP induced testosterone synthesis inhibition, considering scientific, ethical, and economic reasons, we first conducted *in vitro* approaches, and then carry out validation against *in vivo* studies.

Oxidative stress is considered significant factors in various physiological and pathological processes, which can activate multiple intracellular signaling pathways (Ogura and Shimosawa, 2014). When exposed to many environmental chemicals, including DBP, oxidation and antioxidant levels are imbalanced, and then oxidative stress occurs, which can be an important factor affecting reproductive function (Guo et al., 2014). As major contributors to oxidative stress, ROS are double-edged molecules, mediating physiological signaling pathways at low doses, but as a cytotoxic agent at high doses (Martin and Barrett, 2002). Furthermore, related researches have proved that excessive production of ROS is a key trigger of JAK2/STAT3 signaling (Shimizu et al., 2008). The JAK2/STAT3 signaling pathway is a classic intracellular signal transduction pathway, and is involved in many important biological processes. Multiple studies have found that JAK2/STAT3 signaling pathway is associated with numerous male reproductive events, such as gametogenesis generation, sexual development, spermatogonial stem cells renewal, and sperm maturation (Lachance and Leclerc, 2011). It is well known that JAK2/STAT3 is expressed as non-phosphorylated forms under normal and physiological conditions, whereas phosphorylation of JAK2/STAT3 will be instantly accomplished under stressful or pathological situations (Liu et al., 2007). Chong et al. have revealed that administration of a ROS scavenger prior to ischemia inhibit STAT3 activation in cerebral ischemia reperfusion injury, suggesting the suppression of ROS production down-regulates the STAT3 phosphorylation (Lei et al., 2011). Noteworthily, there has been no previous study showing the direct linkage between ROS and the JAK2/STAT3 signaling either in *in vivo* or *in vitro* models of male reproduction. In the present study, p-JAK2/JAK2 and p-STAT3/STAT3 ratios were augmented in both DBP-exposed TM3 cells and mouse testes relative to the Control group, indicating that the JAK2/STAT3 signaling pathway is activated in DBP-induced testosterone synthesis inhibition. Besides, our data showed that the NAC intervention reduced the elevated ROS level and p-JAK2/JAK2 and p-STAT3/STAT3 ratios due to DBP exposure in TM3 cells and mouse testes, indicating that the ROS/JAK2/STAT3 signaling pathway was activated in DBP-induced testosterone synthesis inhibition *in vitro* and *in vivo*.

Mitophagy has been reported to play crucial roles in the regulation of testosterone synthesis. Mitophagy, a specialized form of autophagy, is a double-edged sword for cell survival and death. The moderate mitophagy maintains cellular homeostasis through removing damaged mitochondria. However, excessive mitophagy triggers the activation of cell death pathways through damaging normal mitochondrial. The reduction in MMP results in mitochondrial permeability transition and mitochondrial depolarization, and these changes initiate mitophagy (Cen et al., 2020). LC3 II and Beclin-1 are the marker proteins of autophagy, which can reflect the number of mitophagosomes to some extent (Chen et al., 2010; Vega-Rubín-de-Celis et al., 2020). HSP60, a mitochondrial matrix protein, and TOM20, a mitochondrial outer membrane protein, reflect the total amount of mitochondria (Yang et al., 2019). On the basis that mitophagy is a process that degrades damaged mitochondria, changes in mitochondrial proteins can indirectly reflect the mitophagy level. Lu et al. have demonstrated that glyphosate induces mtROS overproduction to activate parkin-dependent mitophagy, which contributes to the inhibition of testosterone synthesis (Lu et al., 2022). Yang et al. have observed that Benzo[a]pyrene administration remarkably inhibited testosterone synthesis accompanied by ultrastructural impairments of mitochondria and mitophagosome formation in mouse Leydig cells (Yang et al., 2022). Moreover, evidence is accumulating to suggest that the JAK2/STAT3 signaling pathway may play a key role in the mitophagy. Ma et al. have found that pyrroloquinoline quinone lowers denervation-induced skeletal muscle mitophagy via suppressing the JAK2/STAT3 signaling pathway (Ma et al., 2019). Pietzsch et al. have demonstrated that in left ventricular tissue of metastatic melanoma mice, the increased activation of STAT3 upregulates the markers of the mitophagy, indicating that mitophagy may be inhibited by the STAT3 inactivation (Pietzsch et al., 2020). To further validate whether the activation of JAK2/STAT3 signaling pathway engages in mitophagy in DBP-induced testosterone synthesis inhibition, we used AG490, a specific JAK2 protein tyrosine kinase inhibitor, which restrains JAK2 phosphorylation effectively, and blocks its downstream signal transduction and activation of transcription activation factor STAT3. In the present study, DBP-exposed cells and mice exhibited a low MMP, a high LC3 II and Beclin-1 protein expression, and a low HSP60 and TOM20 protein expression compared with the Control group, suggesting that mitophagy was activated in DBP-expose TM3 cells and testes. Interestingly, the AG490 intervention reduced the elevated MMP, LC3 II protein expression, as well as Beclin-1 protein expression ratios, and upregulated the depressed HSP60 protein expression, TOM20 protein expression, and testosterone content due to DBP exposure in TM3 cells and mouse testes, indicating that the restraint of ROS/JAK2/STAT3 signaling pathway could effectively reduce the DBP-induced mitophagy, and in turn to alleviate testosterone synthesis inhibition *in vitro* and *in vivo*.

Apoptosis has been suggested to play a pivotal role in the testosterone synthesis process. Cell apoptosis refers to one sort of cellular initiative procedural death, which occurs under gene control and enzymatic reactions. Mitochondrion-dependent apoptosis pathways may be activated by the excessive ROS production (Wang et al., 2020). Sun et al. have reported that Yangjing Capsule suppresses the apoptosis of MLTC-1 cells, and enhance the production of testosterone (Sun et al., 2018b). Liu et al. have observed that Citrinin reduced testosterone secretion by inducing apoptosis in rat Leydig cells (Liu et al., 2012). Shi et al. have demonstrated that Se can affect the apoptosis of Leydig cells by regulating cellular oxidative stress and apoptosis-related genes, and enhance the testosterone production of Leydig cells (Shi et al., 2017). In recent years, the relation between JAK2/STAT3 signaling pathway and cell apoptosis has been extensively studied. Xia et al. have provided the

evidence that the activity of apoptosis was mediated by JAK2/STAT3 signaling pathway in an early stage after the onset of acute spinal cord injury of rat (Xia et al., 2017). He et al. have revealed that the activation of the JAK2/STAT3 signaling pathway upregulates the apoptosis of renal tubular epithelial cells caused by Hepatitis B virus X protein (He et al., 2013). The similar results were also observed in the present study, after AG490 intervention, the cleaved-caspase-3, Bax, and Cyt-c protein levels were reduced in the DBP-exposed TM3 cells and testes. The EB/AO double fluorescent labeling also showed a relief of apoptosis in the AG490 intervention group. Additionally, the Bcl-2 protein level was augmented in the DBP-exposed TM3 cells and testes by the AG490 intervention. All the data indicated that restraint of ROS/JAK2/STAT3 signaling pathway could effectively reduce the DBP-induced apoptosis, and in turn to alleviate testosterone synthesis inhibition *in vitro* and *in vivo*.

Combining the above discussion, our study provides some limited evidence that DBP can activate ROS/JAK2/STAT3 signaling pathway to induce mitophagy and apoptosis, which in turn promotes testosterone synthesis inhibition *in vitro* and *in vivo*. Thus, searching for efficient treatment of DBP-induced testosterone synthesis inhibition is highly warranted. LYC is the most potent antioxidants among dietary carotenoids, with a singlet-oxygen-quenching ability. Türk et al. reported that because of the antioxidant properties, LYC could abate the incidence of oxidative stress by reacting with and neutralizing free radicals, and subsequently, mitigate the damage that would otherwise be inflicted on testicles and spermatozoon (Türk et al., 2010). In the current study, the high ROS level and low SOD activity were detected in the DBP-exposed group relative to the Control group. Interestingly, those oxidative stress markers were reversed in the LYC cotreatment group, suggesting that LYC relieves DBP-induced oxidative stress both in TM3 cells and testes. Zhao et al. have demonstrated that di (2-ethylhexyl) phthalate causes mitochondrial damage, oxidative damage, and testosterone biosynthesis reduction in Leydig cell via using *in vivo* and vitro approaches, while LYC supplement reversed these changes (Zhao et al., 2022). Xu et al. have observed that LYC inhibits the decrease of testosterone content caused by Benzo[α]pyrene in serum and intratesticular fluids (Xu et al., 2019). In the present study, DBP destroyed the normal ultrastructure, down-regulated the viability of cells, the testosterone content, and the protein expressions of CYP11A1, 17β-HSD, CYP17A1, 3β-HSD, and StAR in TM3 cells and testes, while LYC cotreatment reversed those inhibition, suggesting that LYC relieves DBP-induced testosterone synthesis inhibition both in TM3 cells and testes. Significantly, the LYC reduced the increased p-JAK2/JAK2 and p-STAT3/STAT3 ratios in the DBP-exposed TM3 cells and testes, suggesting that LYC mitigates the activation of JAK2/STAT3 signaling pathway in TM3 cells and testes. Furthermore, Zhu et al. have demonstrated that methyl tert-butyl ether can inhibit testosterone synthesis by inducing ROS generation, mitophagy, and apoptosis at 200 and 300 mM (Zhu et al., 2022). In the current study, the LYC reduced the mitophagy and apoptosis in DBP-exposed testosterone synthesis inhibition. In summary, LYC can suppress ROS/JAK2/STAT3 signaling pathway, and then relieve mitophagy and apoptosis, so that attenuate DBP-induced testosterone synthesis inhibition both *in vivo* and *in vitro*.

5. Conclusion and future perspectives

In conclusion, our study demonstrated that DBP activated ROS/JAK2/STAT3 signaling pathway, promoted mitophagy and apoptosis, which in turn inhibited testosterone synthesis *in vitro* and *in vivo*, while LYC treatment reversed these changes (Fig. 6). Therefore, LYC may serve as a potential therapeutic agent for DBP poisoning. However, under DBP exposure, further detailed and extensive research deserves to be done to define whether LYC is protective against other testicular function, particularly in regulation of spermatogenesis, through this pathway.

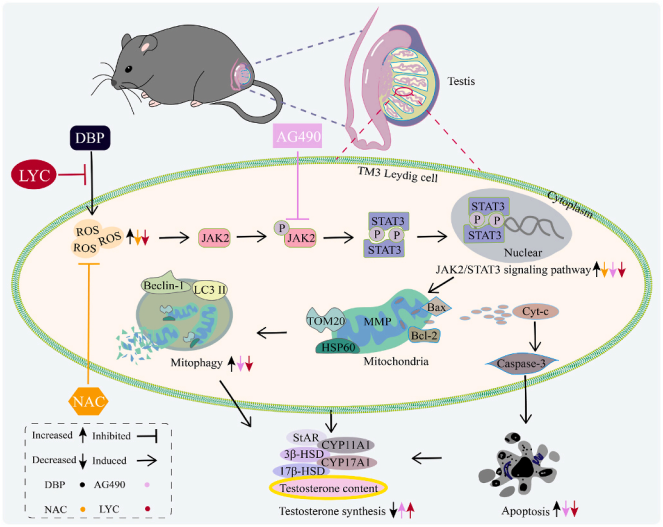

Fig. 6. Schematic diagram of the protective effect of LYC on DBP-induced testosterone synthesis inhibition. The (↑ or ↓) arrow indicates elevation or reduction. Arrows of different colors correspond to changes after different treatment or intervention. Black arrows: DBP exposure. Orange arrows: NAC intervention. Pink arrows: AG490 intervention. Red arrows: LYC treatment. (For interpretation of the references to color in this figure legend, the reader is referred to the Web version of this article.)

CRediT authorship contribution statement

Qi Wang: Conceptualization, Methodology, Data curation, Writing – original draft. **Xia Wu:** Methodology, Validation, Visualization. **Jian Zhang:** Formal analysis. **Miao Song:** Writing – review & editing. **Jiayu Du:** Investigation. **Yilong Cui:** Writing – review & editing. **Yanfei Li:** Supervision, Writing – review & editing.

Declaration of competing interest

The authors declare that they have no known competing financial interests or personal relationships that could have appeared to influence the work reported in this paper.

Data availability

Data will be made available on request.

Acknowledgements

This study was supported by a grant from the National Natural Science Foundation of China (NO. 31872530).

Appendix A. Supplementary data

Supplementary data to this article can be found online at https://doi.org/10.1016/j.fct.2023.113741.

References

Bandeira, A.C.B., Da Silva, T.P., de Araujo, G.R., Araujo, C.M., Da Silva, R.C., Lima, W.G., Bezerra, F.S., Costa, D.C., 2017. Lycopene inhibits reactive oxygen species production in SK-Hep-1 cells and attenuates acetaminophen-induced liver injury in C57BL/6 mice. Chem. Biol. Interact. 263, 7–17.

Basaria, S., Wahlstrom, J.T., Dobs, A.S., 2001. Clinical review 138: anabolic-androgenic steroid therapy in the treatment of chronic diseases. J. Clin. Endocrinol. Metab. 86, 5108–5117.

Cao, L., Zhao, J., Ma, L., Chen, J., Xu, J., Rahman, S.U., Feng, S., Li, Y., Wu, J., Wang, X., 2021. Lycopene attenuates zearalenone-induced oxidative damage of piglet sertoli cells through the nuclear factor erythroid-2 related factor 2 signaling pathway. Ecotoxicol. Environ. Saf. 225, 112737.

Cen, X., Chen, Y., Xu, X., Wu, R., He, F., Zhao, Q., Sun, Q., Yi, C., Wu, J., Najafov, A., Xia, H., 2020. Pharmacological targeting of MCL-1 promotes mitophagy and improves disease pathologies in an Alzheimer's disease mouse model. Nat. Commun. 11, 5731.
Chen, X., Zhou, Q., Leng, L., Chen, X., Sun, Z., Tang, N., 2013. Effects of di(n-butyl) and monobutyl phthalate on steroidogenesis pathways in the murine Leydig tumor cell line MLTC-1. Environ. Toxicol. Pharmacol. 36, 332–338.
Chen, Y., Azad, M.B., Gibson, S.B., 2010. Methods for detecting autophagy and determining autophagy-induced cell death. Can. J. Physiol. Pharmacol. 88, 285–295.
Costa-Rodrigues, J., Pinho, O., Monteiro, P.R.R., 2018. Can lycopene be considered an effective protection against cardiovascular disease? Food Chem. 245, 1148–1153.
Duan, C., Fang, Y., Sun, J., Li, Z., Wang, Q., Bai, J., Peng, H., Liang, J., Gao, Z., 2020. Effects of fast food packaging plasticizers and their metabolites on steroid hormone synthesis in H295R cells. Sci. Total Environ. 726, 138500.
Durairajanayagam, D., Agarwal, A., Ong, C., Prashast, P., 2014. Lycopene and male infertility. Asian J. Androl. 16, 420–425.
Elmigdadi, F., Banihani, I., Banihani, S.A., 2005. Clinico-hormonal correlation of oligospermic patients in the below sea level environment (Jordan Valley). Neuroendocrinol. Lett. 26, 13–18.
Feng, N.X., Feng, Y.X., Liang, Q.F., Chen, X., Xiang, L., Zhao, H.M., Liu, B.L., Cao, G., Li, Y.W., Cai, Q.Y., Mo, C.H., Wong, M.H., 2021. Complete biodegradation of di-n-butyl phthalate (DBP) by a novel Pseudomonas sp. YJB6. Sci. Total Environ. 761, 143208.
Gao, D.W., Wen, Z.D., 2016. Phthalate esters in the environment: a critical review of their occurrence, biodegradation, and removal during wastewater treatment processes. Sci. Total Environ. 541, 986–1001.
Guo, Y., Weck, J., Sundaram, R., Goldstone, A.E., Louis, G.B., Kannan, K., 2014. Urinary concentrations of phthalates in couples planning pregnancy and its association with 8-hydroxy-2'-deoxyguanosine, a biomarker of oxidative stress: longitudinal investigation of fertility and the environment study. Environ. Sci. Technol. 48, 9804–9811.
Han, A., Zou, L., Gan, X., Li, Y., Liu, F., Chang, X., Zhang, X., Tian, M., Li, S., Su, L., Sun, Y., 2018. ROS generation and MAPKs activation contribute to the Ni-induced testosterone synthesis disturbance in rat Leydig cells. Toxicol. Lett. 290, 36–45.
Hauser, R., Meeker, J.D., Duty, S., Silva, M.J., Calafat, A.M., 2006. Altered semen quality in relation to urinary concentrations of phthalate monoester and oxidative metabolites. Epidemiology 17, 682–691.
He, P., Zhang, D., Li, H., Yang, X., Li, D., Zhai, Y., Ma, L., Feng, G., 2013. Hepatitis B virus X protein modulates apoptosis in human renal proximal tubular epithelial cells by activating the JAK2/STAT3 signaling pathway. Int. J. Mol. Med. 31, 1017–1029.
Huang, P.C., Kuo, P.L., Guo, Y.L., Liao, P.C., Lee, C.C., 2007. Associations between urinary phthalate monoesters and thyroid hormones in pregnant women. Hum. Reprod. 22, 2715–2722.
Ignarro, R.S., Vieira, A.S., Sartori, C.R., Langone, F., Rogério, F., Parada, C.A., 2013. JAK2 inhibition is neuroprotective and reduces astrogliosis after quinolinic acid striatal lesion in adult mice. J. Chem. Neuroanat. 48–49, 14–22.
Johnson, K.J., McDowell, E.N., Viereck, M.P., Xia, J.Q., 2011. Species-specific dibutyl phthalate fetal testis endocrine disruption correlates with inhibition of SREBP2-dependent gene expression pathways. Toxicol. Sci. 120, 460–474.
Källsten, L., Almamoun, R., Pierozan, P., Nylander, E., Sdougkou, K., Martin, J.W., Karlsson, O., 2022. Adult exposure to di-N-Butyl Phthalate (DBP) induces persistent effects on testicular cell markers and testosterone biosynthesis in mice. Int. J. Mol. Sci. 23, 8718.
Katsikantami, I., Sifakis, S., Tzatzarakis, M.N., Vakonaki, E., Kalantzi, O.I., Tsatsakis, A. M., Rizos, A.K., 2016. A global assessment of phthalates burden and related links to health effects. Environ. Int. 97, 212–236.
Khashab, F., Al-Saleh, F., Al-Kandari, N., Fadel, F., Al-Maghrebi, M., 2021. JAK inhibition prevents DNA damage and apoptosis in testicular ischemia-reperfusion injury via modulation of the ATM/ATR/Chk pathway. Int. J. Mol. Sci. 22, 13390.
Lachance, C., Leclerc, P., 2011. Mediators of the Jak/STAT signaling pathway in human spermatozoa. Biol. Reprod. 85, 1222–1231.
Lei, C., Deng, J., Wang, B., Cheng, D., Yang, Q., Dong, H., Xiong, L., 2011. Reactive oxygen species scavenger inhibits STAT3 activation after transient focal cerebral ischemia-reperfusion injury in rats. Anesth. Analg. 113, 153–159.
Li, M., Zhang, X., Wang, B., Xu, X., Wu, X., Guo, M., Wang, F., 2018. Effect of JAK2/STAT3 signaling pathway on liver injury associated with severe acute pancreatitis in rats. Exp. Ther. Med. 16, 2013–2021.
Li, W., Jiang, B., Cao, X., Xie, Y., Huang, T., 2017. Protective effect of lycopene on fluoride-induced ameloblasts apoptosis and dental fluorosis through oxidative stress-mediated Caspase pathways. Chem. Biol. Interact. 261, 27–34.
Liu, H., Yao, Y.M., Yu, Y., Dong, N., Yin, H.N., Sheng, Z.Y., 2007. Role of Janus kinase/signal transducer and activator of transcription pathway in regulation of expression and inflammation-promoting activity of high mobility group box protein 1 in rat peritoneal macrophages. Shock 27, 55–60.
Liu, S., Wang, D., Zhang, J., Zhang, D., Gong, M., Wang, C., Wei, N., Liu, W., Wang, Y., Zhao, C., Cui, Y., Hu, D., 2012. Citrinin reduces testosterone secretion by inducing apoptosis in rat Leydig cells. Toxicol. Vitro 26, 856–861.
Lord, T., Aitken, R.J., 2013. Oxidative stress and ageing of the post-ovulatory oocyte. Reproduction 146, R217–R227.
Lu, L., Liu, J.B., Wang, J.Q., Lian, C.Y., Wang, Z.Y., Wang, L., 2022. Glyphosate-induced mitochondrial reactive oxygen species overproduction activates parkin-dependent mitophagy to inhibit testosterone synthesis in mouse leydig cells. Environ. Pollut. 314, 120314.
Ma, T., Zhou, Y., Xia, Y., Jin, H., Wang, B., Wu, J., Ding, J., Wang, J., Yang, F., Han, X., Li, D., 2021. Environmentally relevant perinatal exposure to DBP disturbs testicular development and puberty onset in male mice. Toxicology 459, 152860.
Ma, W., Zhang, R., Huang, Z., Zhang, Q., Xie, X., Yang, X., Zhang, Q., Liu, H., Ding, F., Zhu, J., Sun, H., 2019. PQQ ameliorates skeletal muscle atrophy, mitophagy and fiber type transition induced by denervation via inhibition of the inflammatory signaling pathways. Ann. Transl. Med. 7, 440.
Martin, K.R., Barrett, J.C., 2002. Reactive oxygen species as double-edged swords in cellular processes: low-dose cell signaling versus high-dose toxicity. Hum. Exp. Toxicol. 21, 71–75.
Meng, X., Li, L., An, H., Deng, Y., Ling, C., Lu, T., Song, G., Wang, Y., 2022. Lycopene alleviates titanium dioxide nanoparticle-induced testicular toxicity by inhibiting oxidative stress and apoptosis in mice. Biol. Trace Elem. Res. 200, 2825–2837.
Midzak, A.S., Chen, H., Papadopoulos, V., Zirkin, B.R., 2009. Leydig cell aging and the mechanisms of reduced testosterone synthesis. Mol. Cell. Endocrinol. 299, 23–31.
Nakhaee, S., Dastjerdi, M., Roumi, H., Mehrpour, O., Farrokhfall, K., 2021. N-acetylcysteine dose-dependently improves the analgesic effect of acetaminophen on the rat hot plate test. BMC Pharmacol Toxicol 22, 4.
Ogura, S., Shimosawa, T., 2014. Oxidative stress and organ damages. Curr. Hypertens. Rep. 16, 452.
Pan, G., Hanaoka, T., Yoshimura, M., Zhang, S., Wang, P., Tsukino, H., Inoue, K., Nakazawa, H., Tsugane, S., Takahashi, K., 2006. Decreased serum free testosterone in workers exposed to high levels of di-n-butyl phthalate (DBP) and di-2-ethylhexyl phthalate (DEHP): a cross-sectional study in China. Environ. Health Perspect. 114, 1643–1648.
Petyaev, I.M., 2016. Lycopene deficiency in ageing and cardiovascular disease. Oxid. Med. Cell. Longev., 3218605, 2016.
Pietzsch, S., Ricke-Hoch, M., Stapel, B., Hilfiker-Kleiner, D., 2020. Modulation of cardiac AKT and STAT3 signalling in preclinical cancer models and their impact on the heart. Biochim. Biophys. Acta Mol. Cell Res. 1867, 118519.
Shi, L., Song, R., Yao, X., Ren, Y., 2017. Effects of selenium on the proliferation, apoptosis and testosterone production of sheep Leydig cells in vitro. Theriogenology 93, 24–32.
Shimizu, S., Hiroi, T., Ishii, M., Hagiwara, T., Wajima, T., Miyazaki, A., Kiuchi, Y., 2008. Hydrogen peroxide stimulates tetrahydrobiopterin synthesis through activation of the Jak2 tyrosine kinase pathway in vascular endothelial cells. Int. J. Biochem. Cell Biol. 40, 755–765.
Sun, D., Dong, W., Jin, B., Chen, G., Cai, B., Deng, W., Cui, Y., Jin, Y., 2018a. Mechanisms of Yangjing Capsule in Leydig cell apoptosis and testosterone synthesis via promoting StAR expression. Biol. Pharm. Bull. 41, 1401–1405.
Sun, Y., Shen, J., Zeng, L., Yang, D., Shao, S., Wang, J., Wei, J., Xiong, J., Chen, J., 2018b. Role of autophagy in di-2-ethylhexyl phthalate (DEHP)-induced apoptosis in mouse Leydig cells. Environ. Pollut. 243, 563–572.
Swan, S.H., Main, K.M., Liu, F., Stewart, S.L., Kruse, R.L., Calafat, A.M., Mao, C.S., Redmon, J.B., Ternand, C.L., Sullivan, S., Teague, J.L., 2005. Decrease in anogenital distance among male infants with prenatal phthalate exposure. Environ. Health Perspect. 113, 1056–1061.
Thompson, C., Ross, S., Gaido, K., 2004. Di(n-butyl) phthalate impairs cholesterol transport and steroidogenesis in the fetal rat testis through a rapid and reversible mechanism. Endocrinology 145, 1227–1237.
Tuck, S.P., Francis, R., 2009. Testosterone, bone and osteoporosis. Front. Horm. Res. 37, 123–132.
Türk, G., Ceribaşi, A.O., Sakin, F., Sönmez, M., Ateşşahin, A., 2010. Antiperoxidative and anti-apoptotic effects of lycopene and ellagic acid on cyclophosphamide-induced testicular lipid peroxidation and apoptosis. Reprod. Fertil. Dev. 22, 587–596.
Vega-Rubín-de-Celis, S., Kinch, L., Peña-Llopis, S., 2020. Regulation of Beclin 1-mediated autophagy by oncogenic tyrosine kinases. Int. J. Mol. Sci. 21, 9210.
Wang, C., Qiao, A., Fang, X., Sun, L., Gao, P., Davis, A.R., Liu, S., Luan, F., 2019. Fine mapping of lycopene content and flesh color related gene and development of molecular marker-assisted selection for flesh color in watermelon (citrullus lanatus). Front. Plant Sci. 10, 1240.
Wang, T.S., Coppens, I., Saorin, A., Brady, N.R., Hamacher-Brady, A., 2020. Endolysosomal targeting of mitochondria is integral to BAX-mediated mitochondrial permeabilization during apoptosis signaling. Dev. Cell 53, 627–645.
Wine, R.N., Li, L.H., Barnes, L.H., Gulati, D.K., Chapin, R.E., 1997. Reproductive toxicity of di-n-butylphthalate in a continuous breeding protocol in Sprague-Dawley rats. Environ. Health Perspect. 105, 102–107.
Xia, Y., Chen, J., Ma, T., Meng, X., Han, X., Li, D., 2022. Maternal DBP exposure promotes synaptic formation in offspring by activating astrocytes via the AKT/NF-κB/IL-6/JAK2/STAT3 signaling pathway. Sci. Total Environ. 829, 154437.
Xia, Y., Xia, H., Chen, D., Liao, Z., Yan, Y., 2017. Mechanisms of autophagy and apoptosis mediated by JAK2 signaling pathway after spinal cord injury of rats. Exp. Ther. Med. 14, 1589–1593.
Xu, A., Wang, J., Wang, H., Sun, Y., Hao, T., 2019. Protective effect of lycopene on testicular toxicity induced by Benzo[a]pyrene intake in rats. Toxicology 427, 152301.
Yang, W., Cui, H., Chai, Z., Zou, P., Shi, F., Yang, B., Zhang, G., Yang, H., Chen, Q., Liu, J., Cao, J., Ling, X., Ao, L., 2022. Benzo[a]pyrene inhibits testosterone biosynthesis via NDUFA10-mediated mitochondrial compromise in mouse Leydig cells: integrating experimental and in silico toxicological approaches. Ecotoxicol. Environ. Saf. 244, 114075.
Yang, X., Jiang, T., Wang, Y., Guo, L., 2019. The role and mechanism of SIRT1 in resveratrol-regulated osteoblast autophagy in osteoporosis rats. Sci. Rep. 9, 18424.
Yarrow, J.F., Phillips, E.G., Conover, C.F., Bassett, T.E., Chen, C., Teurlings, T., Vasconez, A., Alerte, J., Prock, H., Jiron, J.M., Flores, M., Aguirre, J.I., Borst, S.E., Ye, F., 2017. Testosterone plus finasteride prevents bone loss without prostate growth in a rodent spinal cord injury model. J. Neurotrauma 34, 2972–2981.

Zhang, X., Qu, N., Zheng, J., Li, Z., Zhang, Y., 2009. Di (n-butyl) phthalate inhibits testosterone synthesis through a glucocorticoid-mediated pathway in rats. Int. J. Toxicol. 28, 448–456.
Zhao, Y., Li, X., Zhang, H., Cui, J., Wang, J., Chen, M., Li, J., 2022. Phthalate-induced testosterone/androgen receptor pathway disorder on spermatogenesis and antagonism of lycopene. J. Hazard Mater. 439, 129689.
Zhu, Q., Zhu, S., Li, Q., Wang, Y., Zheng, D., Chen, C., Ruan, N., Chen, H., Yan, H., Lin, H., Ge, R.S., 2022. Methyl tert-butyl ether inhibits pubertal development of Leydig cells in male rats by inducing mitophagy and apoptosis. Ecotoxicol. Environ. Saf. 232, 113282.